Current Biology *16*, 180–185, January 24, 2006 DOI 10.1016/j.cub.2005.11.074

Report

Septate-Junction-Dependent Luminal Deposition of Chitin Deacetylases Restricts Tube Elongation in the *Drosophila* Trachea

Shenqiu Wang,[1,2] Satish Arcot Jayaram,[1,2] Johanna Hemphälä,[1,2] Kirsten-André Senti,[1] Vasilios Tsarouhas,[1] Haining Jin,[1,3] and Christos Samakovlis[1,*]

[1] Department of Developmental Biology
Wenner-Gren Institute
Stockholm University
Arrhenius Labs E3
S-10691 Stockholm
Sweden

Summary

The function of tubular epithelial organs like the kidney and lung is critically dependent on the length and diameter of their constituting branches. Genetic analysis of tube size control during *Drosophila* tracheal development has revealed that epithelial septate junction (SJ) components and the dynamic chitinous luminal matrix coordinate tube growth. However, the underlying molecular mechanisms controlling tube expansion so far remained elusive. Here, we present the analysis of two luminal chitin binding proteins with predicted polysaccharide deacetylase activities (ChLDs). ChLDs are required to assemble the cable-like extracellular matrix (ECM) and restrict tracheal tube elongation. Overexpression of native, but not of mutated, ChLD versions also interferes with the structural integrity of the intraluminal ECM and causes aberrant tube elongation. Whereas *ChLD* mutants have normal SJ structure and function, the luminal deposition of the ChLD requires intact cellular SJs. This identifies a new molecular function for SJs in the apical secretion of ChLD and positions ChLD downstream of the SJs in tube length control. The deposition of the chitin luminal matrix first promotes and coordinates radial tube expansion. We propose that the subsequent structural modification of chitin by chitin binding deacetylases selectively instructs the termination of tube elongation to the underlying epithelium.

Results and Discussion

An important late step in the morphogenesis of tubular organs is the final acquisition of distinct branch sizes. The fixed length and diameter of tubes dictate the flow rates of the transported gas or liquid and are therefore major determinants of optimal organ function. Several of the genes controlling tube size during organogenesis encode potential regulators of apical membrane and cytoskeletal organization, but the cellular mechanisms measuring and restricting lumen growth are not well understood [1, 2]. In the *Drosophila* airways, a dynamic chitinous extracellular matrix forms inside the developing branches and is required for uniform tube expansion. Loss of the transient chitin cable results in cystic and winding tubes and defects in apical cell shapes and cytoskeletal organization, suggesting that the expanding polysaccharide cable controls tube extension [3, 4]. How does the luminal chitin matrix signal its structural integrity to the epithelium? The lamellar structure and stiffness of arthropod cuticles depends on the arrangement of chitin polymers [β(1–4)-linked N-acetylglucosamine, GlcNAc] in planes of parallel or antiparrallel fibrils through the formation of hydrogen bonds between the chains [5]. Moreover, the rigidity of the *Saccharomyces cerevisiae* spore cell wall requires chitin deacetylases that convert chitin to chitosan, a β(1–4) N-Glucosamine (GlcN) polymer with distinct physical properties [6]. We hypothesized that similar luminal chitin modifications resulting in structural changes of the matrix may control tube length or diameter growth. The fly genome encodes more than 100 putative chitin binding proteins (ChtB, IPR002557) [7], and three of them, encoded by CG8756, CG32209, and CG17905, contain additional Low-Density Lipoprotein Receptor (LDLR, IPR002172) and polysaccharide deacetylase (Polysacc Deac, IPR002509) domains, suggesting that they may be involved in the assembly and maturation of chitin polymers (Figure 1A). We named this protein family ChLDs because of the predicted structure of the encoded proteins, and the CG8756 and CG32209 members were named *vermiform* (*verm*) and *serpentine* (*serp*), respectively, because of the tracheal phenotypes of the mutants (see below). We first analyzed the expression patterns of *verm*, *serp*, and *ChLD3* in wild-type embryos by in situ hybridizations. *verm* and *serp* were expressed in all tracheal cells from stage 12 until the end of embryogenesis, and both genes were also expressed in the epidermis from stage 15 onward (Figure S1 in the Supplemental Data available online). *ChLD3* expression was not detected in the trachea, and it was therefore not analyzed further. To investigate the localization of the Verm protein, we raised antibodies against its C terminus and stained wild-type embryos. We detected Verm inside all tracheal cells from stage 12. Verm deposition into the lumen of the dorsal trunk (DT) commences abruptly at stage 14, followed by all other branches thereafter. By stage 15, the Verm labeling was luminal and lining the apical cell surface of the DT (Figures 1B–1G). This staining was severely reduced to background levels in *verm* mutants. We also used *btl*-GAL4 to express Serp-GFP fusion protein and found it to be secreted into the lumen similarly to endogenous verm (Figure S1).

The dynamic localization of ChLD proteins as well as their predicted structure suggested a role in the assembly of the intraluminal chitinous filament. To determine the function of Verm and Serp, we obtained strong loss-of-function mutations for both genes (see Experimental

*Correspondence: christos@devbio.su.se
[2] These authors contributed equally to this work.
[3] Present address: Department of Genetics, University of Wisconsin, 53706 Madison, Wisconsin.

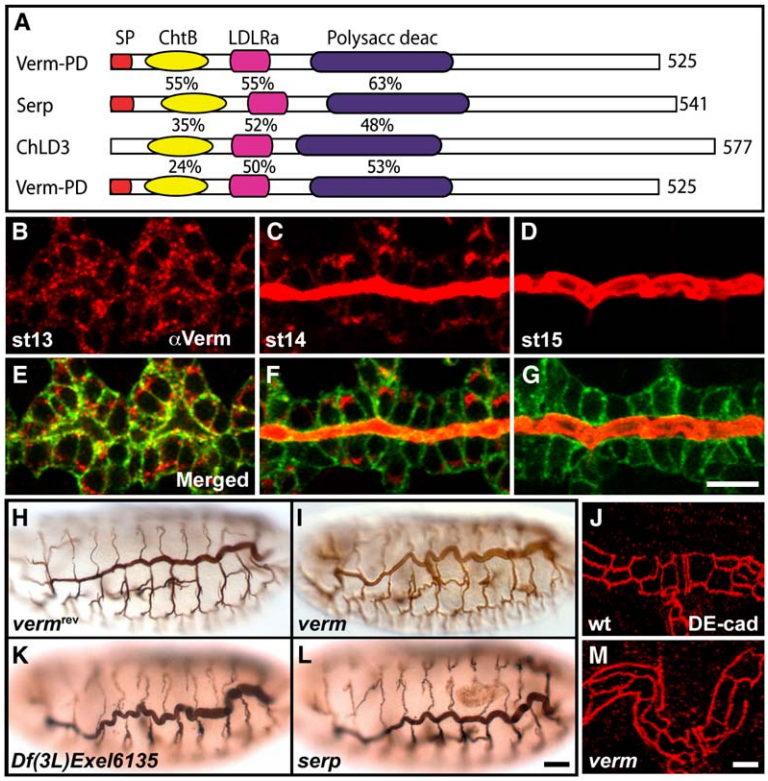

Figure 1. Verm Protein-Localization and Tube-Elongation Phenotypes in *verm* and *serp* Mutants

(A) Sequence comparisons of *Drosophila* *Ch*itin binding, *L*DLRa containing *D*eacetylase (ChLD): Verm-PD (525 aa, isoform D of Verm), Serp (541 aa), and ChLD3 (577 aa). The percentage of identity is shown for each predicted domain. SP denotes signal peptide; ChtB denotes chitin binding domain; LDLRa denotes low-density lipoprotein receptor domain class A; and Polysacc deac denotes polysaccharide deacetylase domain.

(B–G) Confocal sections of DTs of *btl*-GAL4/UAS-*GFP-CAAX* embryos labeled with anti-Verm (red) and anti-GFP (green). Verm protein was first detected inside the tracheal cells at stage 13 (B, E) and then deposited into the tracheal lumen from stage 14 onward (C, F and D, G). Scale bar: 10 μm.

(H–I, K–L) Lateral view of stage 16 *verm* (I) and $serp^{Ex10}$ mutant (L) embryos labeled with 2A12. Lack of phenotype in a *verm* reverted excision allele (H). *Df(3L)Exel6135* embryos (K), lacking both genes, display further tube elongations than either single mutant. Scale bar: 25 μm.

(J, M) Confocal projections of DTs of stage-16 wild-type (J) and *verm* mutants (M) labeled for DE-cad to visualize the apical-cell circumference. *verm* mutants show irregular and elongated cell shapes compared to wild-type. Scale bar: 5 μm.

Procedures and Figure S1). Stage-16 *verm* mutant embryos stained for the luminal 2A12 antigen display excessive elongation and convolutions of the DTs, which become gradually more pronounced in later stages. This defect becomes largely ameliorated in mutants expressing UAS-*verm* in the trachea, suggesting that *verm* restricts tube elongation (Figure S1). We also detected similarly elongated DT tubes in *serp* mutant embryos (Figures 1I and 1L). In addition, *Df(3L)Exel6135* embryos, lacking ten genes including *verm* and *serp*, show more severe tube-overextension phenotypes than either single mutant (Figure 1K). These mutants also displayed a slight diametric overgrowth in the DT, suggesting that the removal of both ChLDs, or other genes in their neighborhood, may also influence the restriction of radial tube growth. The analysis of *verm* and *serp* embryos labeled with anti-DE-Cadherin antibodies also revealed overstretched cellular profiles (Figures 1J and 1M and data not shown). This indicates that both *verm* and *serp* are required to halt tube elongation and co-ordinate apical cell extensions at late stage 15. The aggravated phenotype of embryos deficient for both proteins suggests that they may cooperate in that task.

Do the tube-length defects in the mutants correlate with phenotypes in the assembly and structure of the luminal matrix? We first analyzed luminal chitin assembly by a fluorescent chitin binding protein (ChtB) and a fluorescent chitin binding lectin (WGA) [3]. Both reagents revealed a cylindrical structure of tightly packed luminal chitin polymers in the wild-type. In homozygous *verm* and hemizygous *serp* embryos, this structure appeared diffuse and expanded radially already at stage 15. By stage 16, its labeling intensity was severely reduced in the DTs compared to the wild-type (Figures 2A–2H). Analysis of transverse transmission electron microscopy (TEM) sections of wild-type DTs at stage 16 reveals a homogenously packed luminal matrix of parallel fibrils. The orientation and assembly of the fibrils is distorted in *verm* mutants, indicating that ChLDs organize intraluminal chitin packing (Figures 2I and 2J). The formation of the luminal matrix depends on the chitin synthetase encoded by *kkv* [8]. In *kkv* mutants, the chitinous cable is absent and the tubes first fail to expand their diameter and later become over elongated and convoluted [3]. The tube phenotypes of *kkv verm* double mutants were identical to the ones of *kkv*, indicating that chitin synthesis is a prerequisite for ChLD function (not shown). In addition, the luminal Verm staining was severely disrupted in *kkv* mutants (Figures 2K and 2L). Whereas early events of tracheal cuticle assembly, like the apical deposition of the epicuticle layers at early stage 16, were unaffected in *verm* mutants (see below), cuticular abnormalities were detected in DT cross-sections at late stage 16. These include irregular taenidia, reduced procuticle deposition, and aberrant apical membranes (Figures 2M and 2N), revealing an additional, later role of Verm in tracheal cuticle assembly. The above data argue that ChLDs are primarily required to form or preserve the tight texture of the chitinous luminal cable and that their function and localization require *kkv* and its product chitin.

To further analyze the functional potential of ChLD proteins, we overexpressed native and GFP-tagged versions of Verm and Serp in the trachea and assessed the phenotypes in embryos stained for the ChtB reagent or 2A12 (Figures 3B–3F and data not shown). Expression of either transgene caused distortion of the filamentous

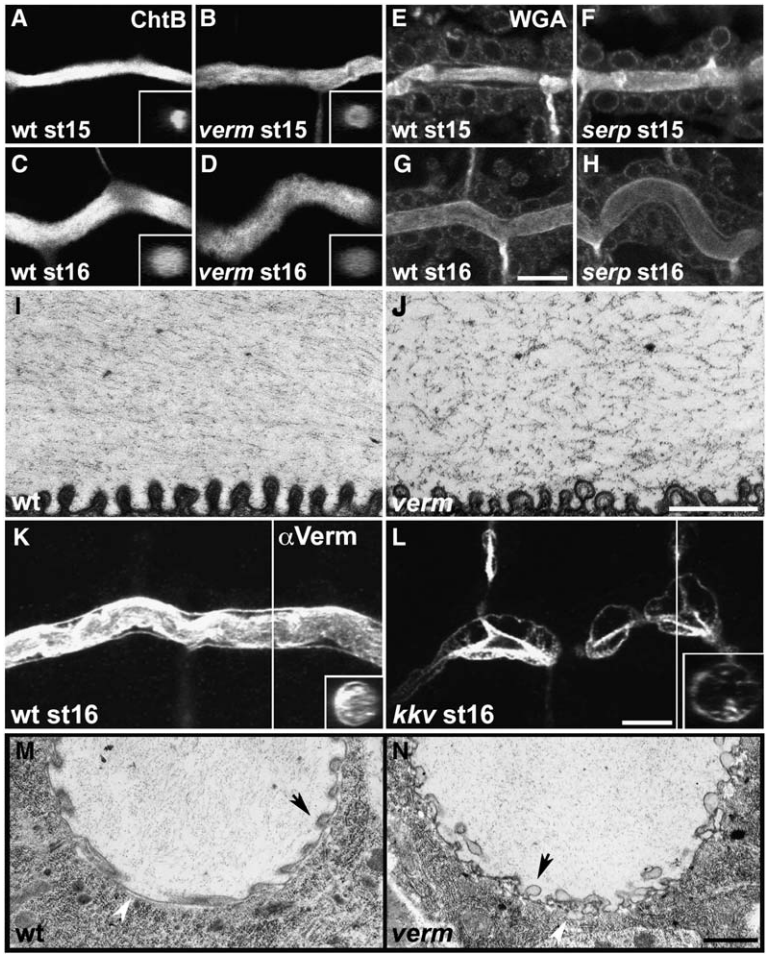

Figure 2. ChLDs Control the Structure of the Chitinous Luminal Matrix

(A–D) Confocal sections of wild-type (A, C) and *verm* mutant (B, D) DTs labeled with an FITC-conjugated chitin binding probe (ChtB). All inserts display y-z projections. A dynamic filamentous cable is detected in the lumen of wild-type stage-15 and -16 embryos. The structure is diffuse and expanded in the mutants.

(E–H) Confocal sections of WGA-labeled wild-type (E, G) and *serp*^{d03931}/*Df(3L)XS705* mutant (F, H) DTs show the chitin cable relative to the epithelial cell membranes and nuclei, which are also labeled by the lectin. Intraluminal WGA labeling is expanded and less dense already at stage 15 in the mutants. Scale bar in (A)–(H): 10 μm.

(I–J) TEMs of transverse sections from stage-16 wild-type (I) and *verm* mutant (J) DTs show irregular taenidia and aberrant fibrous luminal material in the mutants. Scale bar: 1 μm.

(K–L) Confocal sections of Verm-labeled DTs of stage-16 wild-type (K) and *kkv* (L) embryos. Verm localization along the apical membranes and in the lumen is disrupted in *kkv* mutants. Scale bar: 5 μm.

(M–N) TEMs of DT cross-sections from late stage-16 wild-type (M) and *verm* mutants. (N) Mutants show cuticular (black arrows) and apical membrane defects (white arrowheads). Scale bar: 1 μm.

texture and a reduction in the staining intensity of the chitin cable. Whereas native Verm causes lesser effects, Serp and both GFP-tagged versions induce more-pronounced phenotypes. Moreover, the tube-overgrowth and -winding phenotypes in the tracheal branches were proportional to the severity of the intraluminal matrix defect (Figures 3D–3F). Thus, ChLD-induced changes in filament structure play an instructive role in tube elongation.

To dissect the function of the three predicted domains of Serp in this assay, we generated transgenic embryos expressing GFP-tagged versions lacking each of the motifs (Figure 3A). Tracheal expression of Serp-ΔChtB-GFP or Serp-ΔLDLR-GFP did not cause any detectable luminal or tube-extension phenotype, indicating that both domains are necessary for the function of Serp in tube length control (Figures 3G, 3H, 3J, and 3K). Expression of Serp-ΔDeac-GFP did not affect tube elongation either, but, surprisingly, we found that the protein does not become secreted but accumulates inside the tracheal cells (Figures 3I and 3L). Thus, the deacetylase domain harbors motifs required for Serp luminal secretion. The failure of the deletion constructs to cause phenotypes argues against antimorphic effects of the ChLD-GFP proteins and indicates that all three predicted domains are required for tracheal Serp function. Overexpression of the ChLDs leads to similar luminal and tube-elongation phenotypes as their loss of function, suggesting that both lack of as well as increased levels of chitin modifications result in similar effects.

The analysis of several *Drosophila* mutants with overgrown tracheal tubes similar to *verm* and *serp* embryos demonstrated that paracellular septate junction (SJ) components are required for halting lumen overgrowth [9–14]. Two different molecular mechanisms were proposed to account for the tube-overextension phenotypes in SJ mutants: First, SJ-associated proteins like Scribble and Discs Large may restrict the activity of apical-membrane growth-promoting factors like Crb and DaPKC during tube growth [13], and second, SJ functions may be required in luminal matrix assembly and thereby indirectly regulate tube expansion [3] (see Figure S2). Is there a mechanistic link between the function of SJs and ChLDs in tube length control? We first examined whether ChLDs are required for the assembly of SJs. We analyzed *Df(3L)Exel6135* and *verm* mutant embryos in three different assays. First, we stained with antibodies against the SJ markers Neurexin and FasIII (Figures 4A and 4B and data not shown). Secondly, we analyzed DT crossections of *verm* mutants for the ladder-like SJ structure by TEM (Figures 4G and 4H). Finally, we tested the function of the paracellular barrier by Dextran injections [15] (Figures 4C–4F). *ChLD* mutants were indistinguishable from wild-type in all three experiments, arguing that ChLD does not affect SJ structure or function. Is Verm affected in SJ mutants?

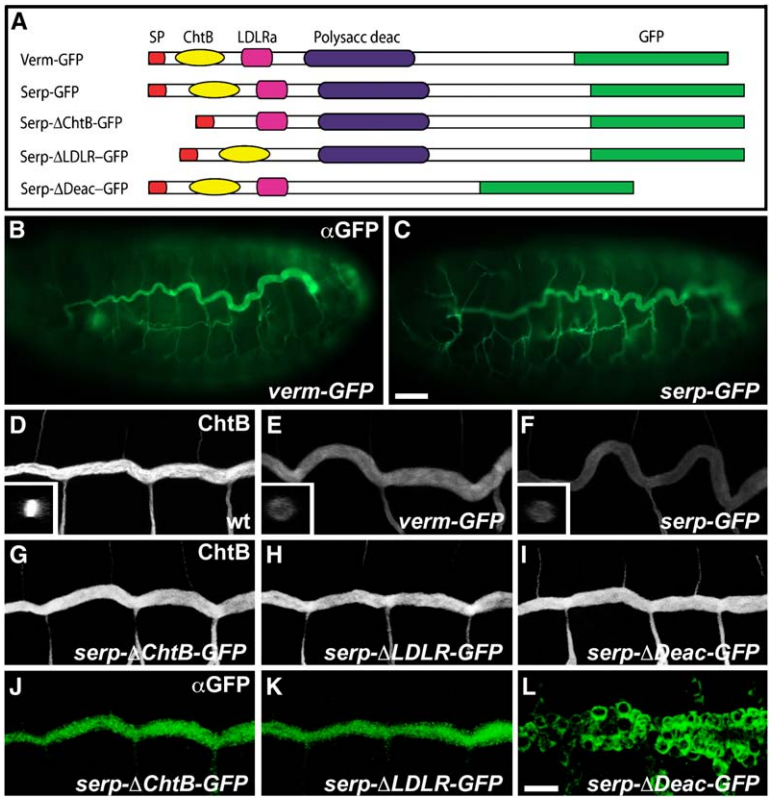

Figure 3. Overexpression of Full-Length, But Not Mutated, ChLD Proteins Disrupts the Chitin Cable and Causes Tube Elongation

(A) Diagram of GFP-tagged ChLDs and deletion versions.

(B–C) GFP labeling of stage-16 *btl*-GAL4/UAS-*verm-GFP* (B) and *btl*-GAL4/UAS-*serp-GFP* (C) embryos reveal elongated tubes. Scale bar: 25 μm.

(D–F) DT confocal projections of wild-type (D), *btl*-GAL4/UAS-*verm-GFP* (E), and *btl*-GAL4/UAS-*serp-GFP* (F) stage-16 embryos labeled with fluorescent ChtB. The reduction of labeling intensity and cable texture distortion is proportional to the tube-elongation phenotypes.

(G–L) ChtB and GFP double labeling of *btl*-GAL4/UAS-*serp-ΔChtB-GFP* (G), *btl*-GAL4/UAS-*serp-ΔLDLR-GFP* (H), and *btl*-GAL4/UAS-*serp-ΔDeac-GFP* (I) embryos. None of the mutated versions caused tracheal phenotypes (G–I). In contrast to Serp-ΔChtB-GFP (J) and Serp-ΔLDLR-GFP (K), Serp-ΔDeac-GFP protein is retained inside the tracheal cells (L). Scale bar in (D)–(L): 10 μm.

We analyzed the localization of Verm in mutants for the α subunit of the Na/K-ATPase (*Atpα*) [16]. In these embryos, Verm is retained inside the tracheal cells at stage 15, whereas its luminal abundance is strongly reduced and becomes gradually undetectable at stage 16. This defect in Verm luminal secretion is accompanied by only a subtle decrease in the luminal 2A12 staining (Figures 4I–4T). We detected the same phenotypes of aberrant Verm intracellular accumulation and strongly reduced luminal levels in *sinu* (Claudin) [14] and *lac* (*bulb*) [11] mutants, suggesting that Verm luminal secretion depends on the assembly or maintenance of the SJ structure (Figure S3). The defect of Verm intracellular retention and luminal stabilization in SJ mutants is unlikely to reflect a general block of apical secretion because neither the 2A12 marker nor the luminal ZP-protein Pio [17] showed defects in luminal accumulation at stage 15 (Figures 4J and 4N and data not shown). The distinct luminal-deposition phenotypes demonstrate a new function for the transepithelial barrier junctions in the apical secretion of Verm. Moreover, these apical secretion defects provide molecular evidence that ChLDs act downstream of the SJs to regulate tube size. The sorting signal required for apical targeting via SJs is presently unknown, and its identification may be aided by the dissection of the role of sequences in the Deacetylase domain in luminal secretion.

The phenotypic analysis of known tracheal-tube-size mutants unveiled an instrumental role of the chitinous extracellular matrix structure in orchestrating branch dimensions. The assembly and growth of the chitin cable first coordinates the radial expansion of the tubes. Subsequent modifications in chitin fibril structure by secreted ChLDs instruct the underlying epithelium to terminate tube elongation. Thus, dynamic structural changes of the luminal matrix may be sensed independently to determine diametric growth and tube elongation (Figure 4U). Given the predicted structure of ChLDs, such changes may involve chitin deacetylation and consequently the extent of hydrogen bonding between chitin fibers and their packing. The similar loss- and gain-of-function ChLD phenotypes suggest that the distinct level of chitin modification and the expected changes in matrix rigidity monitor tube elongation. Luminal fibrillar ECM structures have been described in a vertebrate angiogenesis model [18], and our genetic analysis provides a first mechanistic view on distinct functions of the luminal ECM in tube size control.

Experimental Procedures

Drosophila Strains

The *KG07819* P element is inserted 100 bp upstream of the *verm* translation start site [19]. The XP type P element *d03931* is inserted in the *serp* 5′ UTR, 228 bp upstream of the first ATG [20]. Imprecise and precise excisions of both insertions each yielded several viable and lethal strains (noncomplementing *Df(3L)XS543*, *Df(3L)XS705*, and *Df(3L)Exel6135*) [21], which remove both *verm* and *serp* [22]. The revertants $verm^{ex245}$ and $serp^{ex7}$ and the lethals $verm^{KG07819}$ (*verm* in text), $serp^{ex10}$, and $serp^{d03931}$ lines (*serp* in text) were used for phenotypic analysis. To analyze the double-mutant phenotype, we recombined $verm^{KG07819}$ with $kkv^{l(3)s017909}$ [3]. Other mutations used are $sinu^{06524}$ [14], $bulb/lac^{k11012b}$ [10, 11], kkv^{DZ8} [8], and $Atp\alpha^{s067611}$ [16]. *btl*-GAL4 and a *btl*-GAL4 UAS-*GFP-CAAX* recombinant, both on the second chromosome, were used for overexpression and to label tracheal cells. Appropriate *lacZ*- or *gfp*-marked CyO and TM3 balancers were used.

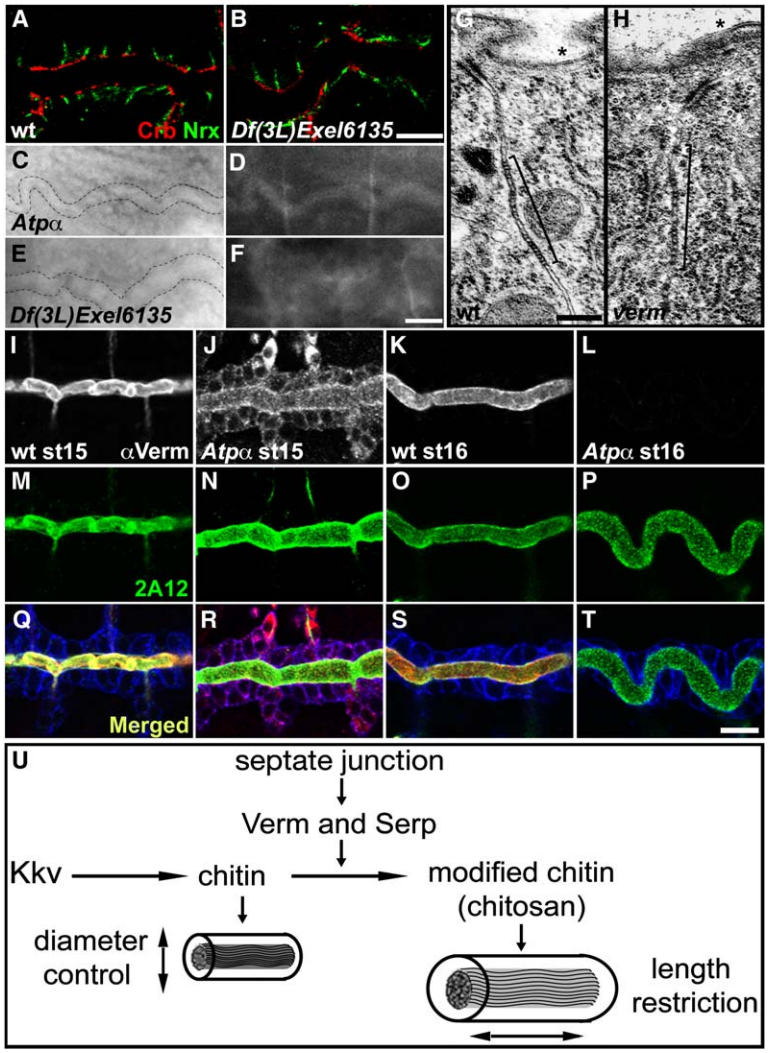

Figure 4. ChLDs Act Downstream of the SJs in Tube-Elongation Restriction

(A–B) Confocal DT sections of wild-type (A) and *Df(3L)Exel6135* mutants (B) stained for Crb and Nrx. The localization of Nrx is not affected in the mutants. Scale bar: 10 μm

(C–F) DIC and fluorescent images of *Atpα* (C–D) and *Df(3L)Exel6135* (E–F) embryos injected with Rhodamine-labeled 10 kDa Dextran. Intraluminal fluorescence is only detected in *ATPα* mutants. The DTs are highlighted with broken lines in (C) and (E). Scale bar: 10 μm.

(G–H) TEMs of DT cross-sections of stage-16 wild-type (G) and *verm* mutants (H). Neither the SJ ladder (brackets) nor the early steps of epicuticle formation (asterisk) appear defective in the mutants. Scale bar: 200 nm.

(I–T) Confocal sections of DTs of wild-type (I, K, M, O, Q, S) and *Atpα* mutants (J, L, N, P, R, T) expressing GFP-CAAX in the trachea stained for Verm, 2A12, and GFP. Verm remains intracellular in *Atpα* embryos at stage 15 and is undetectable at stage 16. Scale bar: 10 μm.

(U) A model for the sequential generation and function of the dynamic chitinous matrix during tube growth. First-chitin assembly coordinates radial expansion of the lumen during stage 14. Subsequent structural modification of the chitin cable instructs the termination of tube elongation to the epithelium at stage 16. Structural changes in the chitin cable may be perceived through its adhesion to the epithelium or by specific receptors on the cell surface.

Molecular Biology

Verm encodes four putative protein isoforms deriving from alternative splicing: verm-PA, -PB, -PC, and -PD [23]. They all share the same predicted protein domains (Figure 1) except Verm-PA, which contains an additional predicted chitin binding motif. Verm antisera were generated against a protein corresponding to aa 377–570 of Verm-PA (and shared by all isoforms) fused to the 6× HisTag from pRSETB. Protein purified on Ni-NTA resin was injected into guinea pigs.

UAS-*verm* and *serp* transgenes were generated by subcloning the inserts of RE29613 for *verm-PD* and RE22242 for *serp* into pUAST. PCR amplicons comprising the 5′ UTR and coding regions of the above cDNAs were subcloned in frame with a C-terminal EGFP tag into pUAST to construct fluorescent variants. Serp domain constructs were made by PCR amplification and subcloning into pUAST: *serp-ΔChtB-GFP* lacks aa 46–105, *serp-ΔLDLR-GFP* aa 124–161, and *serp-ΔDeac-GFP* aa 196–331. All PCR-derived inserts were confirmed by sequencing.

Digoxigenin-labeled RNA probes were transcribed from AT19763 (*verm*), RE22242 (*serp*), and RE01566 (*ChLD3*) and hybridized to embryos according to [24]. Antibody, chitin stainings and TEM were performed as in [3, 16]. Anti-α-spectrin was used at 1/10 (clone 3A9; DSHB) and mouse anti-GFP at 1/1000 (clone 20, Sigma). Polyclonal guinea pig anti-Verm was used at 1/500. For dye-permeability assays, Rhodamine-B-conjugated 10 kDa Dextran was injected into live late-stage embryos and examined on a fluorescence microscope [15].

Supplemental Data

Supplemental Data include three figures and are available with this article online at: http://www.current-biology.com/cgi/content/full/16/2/180/DC1/.

Acknowledgments

We thank S. Luschnig and M. Krasnow for communicating their results before publication and I. Grannel and M Björk for excellent technical assistance. We also thank M. Affolter, the Developmental Studies Hybridoma Bank (DSHB), and the Bloomington and the Exelixis/Harvard stock centers for fly strains and antibodies. K.A.S. is supported by an EMBO fellowship. The work was supported by grants from VR, SSF, and WCN to C.S.

Received: October 13, 2005
Revised: November 28, 2005
Accepted: November 28, 2005
Published: January 23, 2006

References

1. Lubarsky, B., and Krasnow, M.A. (2003). Tube morphogenesis: Making and shaping biological tubes. Cell *112*, 19–28.
2. Hogan, B.L., and Kolodziej, P.A. (2002). Organogenesis: Molecular mechanisms of tubulogenesis. Nat. Rev. Genet. *3*, 513–523.

3. Tonning, A., Hemphala, J., Tang, E., Nannmark, U., Samakovlis, C., and Uv, A. (2005). A transient luminal chitinous matrix is required to model epithelial tube diameter in the Drosophila trachea. Dev. Cell *9*, 423–430.
4. Devine, W.P., Lubarsky, B., Shaw, K., Luschnig, S., Messina, L., and Krasnow, M.A. (2005). Requirement for chitin biosynthesis in epithelial tube morphogenesis. Proc. Natl. Acad. Sci. USA *102*, 17014–17019. Published online November 15, 2005. 10.1073/pnas.0506676102.
5. Merzendorfer, H., and Zimoch, L. (2003). Chitin metabolism in insects: Structure, function and regulation of chitin synthases and chitinases. J. Exp. Biol. *206*, 4393–4412.
6. Christodoulidou, A., Briza, P., Ellinger, A., and Bouriotis, V. (1999). Yeast ascospore wall assembly requires two chitin deacetylase isozymes. FEBS Lett. *460*, 275–279.
7. Magkrioti, C.K., Spyropoulos, I.C., Iconomidou, V.A., Willis, J.H., and Hamodrakas, S.J. (2004). cuticleDB: A relational database of Arthropod cuticular proteins. BMC Bioinformatics *5*, 138.
8. Ostrowski, S., Dierick, H.A., and Bejsovec, A. (2002). Genetic control of cuticle formation during embryonic development of Drosophila melanogaster. Genetics *161*, 171–182.
9. Behr, M., Riedel, D., and Schuh, R. (2003). The claudin-like megatrachea is essential in septate junctions for the epithelial barrier function in Drosophila. Dev. Cell *5*, 611–620.
10. Beitel, G.J., and Krasnow, M.A. (2000). Genetic control of epithelial tube size in the Drosophila tracheal system. Development *127*, 3271–3282.
11. Llimargas, M., Strigini, M., Katidou, M., Karagogeos, D., and Casanova, J. (2004). Lachesin is a component of a septate junction-based mechanism that controls tube size and epithelial integrity in the Drosophila tracheal system. Development *131*, 181–190.
12. Paul, S.M., Ternet, M., Salvaterra, P.M., and Beitel, G.J. (2003). The Na+/K+ ATPase is required for septate junction function and epithelial tube-size control in the Drosophila tracheal system. Development *130*, 4963–4974.
13. Wu, V.M., and Beitel, G.J. (2004). A junctional problem of apical proportions: epithelial tube-size control by septate junctions in the Drosophila tracheal system. Curr. Opin. Cell Biol. *16*, 493–499.
14. Wu, V.M., Schulte, J., Hirschi, A., Tepass, U., and Beitel, G.J. (2004). Sinuous is a Drosophila claudin required for septate junction organization and epithelial tube size control. J. Cell Biol. *164*, 313–323.
15. Lamb, R.S., Ward, R.E., Schweizer, L., and Fehon, R.G. (1998). Drosophila coracle, a member of the protein 4.1 superfamily, has essential structural functions in the septate junctions and developmental functions in embryonic and adult epithelial cells. Mol. Biol. Cell *9*, 3505–3519.
16. Hemphala, J., Uv, A., Cantera, R., Bray, S., and Samakovlis, C. (2003). Grainy head controls apical membrane growth and tube elongation in response to Branchless/FGF signalling. Development *130*, 249–258.
17. Jazwinska, A., Ribeiro, C., and Affolter, M. (2003). Epithelial tube morphogenesis during Drosophila tracheal development requires Piopio, a luminal ZP protein. Nat. Cell Biol. *5*, 895–901.
18. Folkman, J., and Haudenschild, C. (1980). Angiogenesis in vitro. Nature *288*, 551–556.
19. Bellen, H.J., Levis, R.W., Liao, G., He, Y., Carlson, J.W., Tsang, G., Evans-Holm, M., Hiesinger, P.R., Schulze, K.L., Rubin, G.M., et al. (2004). The BDGP gene disruption project: Single transposon insertions associated with 40% of Drosophila genes. Genetics *167*, 761–781.
20. Thibault, S.T., Singer, M.A., Miyazaki, W.Y., Milash, B., Dompe, N.A., Singh, C.M., Buchholz, R., Demsky, M., Fawcett, R., Francis-Lang, H.L., et al. (2004). A complementary transposon tool kit for Drosophila melanogaster using P and piggyBac. Nat. Genet. *36*, 283–287.
21. Parks, A.L., Cook, K.R., Belvin, M., Dompe, N.A., Fawcett, R., Huppert, K., Tan, L.R., Winter, C.G., Bogart, K.P., Deal, J.E., et al. (2004). Systematic generation of high-resolution deletion coverage of the Drosophila melanogaster genome. Nat. Genet. *36*, 288–292.
22. Ito, N., and Rubin, G.M. (1999). gigas, a Drosophila homolog of tuberous sclerosis gene product-2, regulates the cell cycle. Cell *96*, 529–539.
23. Celniker, S.E., Wheeler, D.A., Kronmiller, B., Carlson, J.W., Halpern, A., Patel, S., Adams, M., Champe, M., Dugan, S.P., Frise, E., et al. (2002). Finishing a whole-genome shotgun: Release 3 of the Drosophila melanogaster euchromatic genome sequence. Genome Biol. *3*. RESEARCH0079. Published online December 23, 2002. 10.1186/gb-2002-3-12-research0079.
24. Lehmann, R., and Tautz, D. (1994). In situ hybridization to RNA. Methods Cell Biol. *44*, 575–598.